Laukkanen, Olli Ville; Winter, H. Henning; Seppälä, Jukka

Characterization of physical aging by time-resolved rheometry

Published in:
Rheologica Acta

DOI:
10.1007/s00397-018-1114-8

Published: 01/11/2018

Document Version
Peer-reviewed accepted author manuscript, also known as Final accepted manuscript or Post-print

Characterization of physical aging by time-resolved rheometry: Fundamentals and application to bituminous binders

Olli-Ville Laukkanen[*,1,2], *H. Henning Winter*[1], *and Jukka Seppälä*[2]

[1] *Department of Polymer Science and Engineering and Department of Chemical Engineering, University of Massachusetts, Amherst, Massachusetts 01003, United States*

[2] *Department of Chemical and Metallurgical Engineering, School of Chemical Engineering, Aalto University, P.O. Box 16100, 00076 Aalto, Finland*

* Corresponding author, email: olaukkanen@mail.pse.umass.edu

Abstract Physical aging is a ubiquitous phenomenon in glassy materials and it is reflected, for example, in the time evolution of rheological properties under isothermal conditions. In this paper, time-resolved rheometry (TRR) is used to characterize this time-dependent rheological behavior. The fundamentals of TRR are briefly reviewed, and its advantages over the traditional Struik's physical aging test protocol are discussed. In the experimental section, the TRR technique is applied to study physical aging in bituminous binders. Small-diameter parallel plate (SDPP) rheometry is employed to perform cyclic frequency sweep (CFS) experiments over extended periods of time (from one to 8.6 days). The results verify that the mutation of rheological properties is relatively slow during physical aging (mutation number $N'_{mu} << 1$), thus allowing rheological measurements on a quasi-stable sample. The effects of temperature, crystallinity and styrene-butadiene-styrene (SBS) polymer modification on the physical aging of bitumen are evaluated. The time-aging time superposition is found to be valid both for unmodified and for polymer modified bitumen. Vertical shifts are necessary, in addition to horizontal time-aging time shifts, to generate smooth master curves for highly SBS modified bitumen.

Keywords: Physical aging, Sample mutation, Time-resolved rheometry, Time-aging time superposition, Bitumen

Introduction

Physical aging refers to structural relaxation of the glassy state toward the metastable equilibrium amorphous state (Hodge 1995), and it is driven by the attempt to achieve equilibrium density through configurational rearrangements on a molecular scale (Simon 2001). Physical aging is accompanied by changes in almost all physical properties, at both the macrostructural (bulk) and microstructural (molecular) scale (Struik 1977; Hodge 1995; Hutchinson 1995). Among many other characterization techniques (dilatometry, differential scanning calorimetry, various spectroscopic and scattering techniques, etc.), physical aging can be conveniently detected by rheology (McKenna 2013). In particular, it is common to use the so-called Struik's protocol (Struik 1977) to study the evolution of creep response during physical aging.

While the effects of physical aging on the creep response have been widely studied, much less attention has been paid to the evolution of dynamic viscoelastic properties in physically aging materials. Even so, the effects of physical aging on the dynamic viscoelastic properties have been studied in a number of glassy homo- and copolymers during the past few decades (Kovacs et al. 1963; Guerdoux et al. 1984; Pixa et al. 1985; Cavaille et al. 1986; Wang and Ogale 1989; Haidar and Smith 1990; Ricco and Smith 1990; Venditti and Gillham 1992a, b, Beiner et al. 1994b, a; Brennan and Feller III 1995; Delin et al. 1996; Alcoutlabi and Martinez-Vega 1999; Araki et al. 2001b, a; Araki and Masuda 2001; Drozdov 2001; Drozdov and Dorfmann 2003; Cugini and Lesser 2015; Tian et al. 2015). It is noteworthy, however, that to the best of our knowledge, no such investigations have been conducted on small-molecule (non-polymeric) glass-forming liquids. Furthermore, the fundamentals and possible limitations of using dynamic mechanical experiments to characterize physical aging have not been discussed in detail before.

In 1994, Mours and Winter introduced a novel framework for studying viscoelastic materials that undergo changes during rheological characterization (Mours and Winter 1994). This approach is known as time-resolved rheometry (TRR) and it involves the measurement of time-dependent dynamic viscoelastic properties at various angular frequencies. Since its introduction, the TRR technique has been employed in the rheological characterization of a wide variety of transient materials, including polymers during cross-linking (Mours and Winter 1996, 1998; De Rosa et al. 1997; Kaushal and Joshi 2014; Zhang et al. 2014), crystallization (Pogodina and Winter 1998), shear-induced phase ordering (Mandare and Winter 2007), phase separation (Polios et al. 1997), and thermal/thermo-oxidative degradation (Filippone et al. 2015a, b; Kruse and Wagner 2016; Salehiyan et al. 2017). In particular, TRR is often used to detect the gel point (Winter 2016).

In this article, we introduce TRR as a powerful technique to characterize physical aging in glassy materials. The fundamentals of TRR are reviewed, and the advantages of this method over the classical Struik's protocol are discussed. As a practical application, we use the TRR technique to analyze physical aging in various types of bituminous binders. In particular, the effects of temperature, crystallinity and polymer modification are studied. The results of these analyses are of great importance especially to the asphalt paving industry as the physical aging of bituminous binders has a major impact on the durability of asphalt pavements (Iliuta et al. 2004b, a; Soenen et al. 2004; Yee et al. 2006; Zhao and Hesp 2006; Hesp et al. 2007, 2009a, b; Evans et al. 2011; Bahia et al. 2012; Paul Togunde and Hesp 2012; Freeston et al. 2015).

Theory

Sample mutation

The term 'mutation' is used as a general expression for the changes that affect the molecular mobility, and hence the relaxation patterns of the investigated material (Winter et al. 1998). The mutation time τ_{mu} is defined as the characteristic time for the rate of change in the material (Mours and Winter 1994):

$$\tau_{mu} = \left[\frac{1}{g}\left|\frac{\partial g}{\partial t}\right|\right]^{-1} \quad (1)$$

The change is not measured directly but indirectly through the property of interest g, which has to be specified for each type of experiment. τ_{mu} is defined as the time which is required for a $(1/e)$-change of property g at the instantaneous rate of change $\partial g/\partial t$. Furthermore, the mutation number N_{mu} can be calculated considering the experimental time Δt (Winter et al. 1988):

$$N_{mu} = \frac{\Delta t}{\tau_{mu}} \quad (2)$$

This parameter estimates the change during an experiment, i.e. N_{mu} = experimental time / mutation time. For small N_{mu}, the mutation is small enough to be negligible in the analysis of an experiment.

Time-resolved rheometry (TRR)

It is usually desirable to investigate transient samples specifically by dynamic oscillatory experiments since the experimental time is shorter than in comparable steady experiments and different relaxation modes can be studied almost independently of each other (Winter et al. 1998). In small-amplitude oscillatory shear (SAOS) experiments, the sample is subjected to a sinusoidal strain or stress, and dynamic viscoelastic properties such as the storage modulus G' and loss modulus G'' are measured. The experimental time Δt in this type of measurement is defined by the time required by the rheometer to take a data point at a specified angular frequency ω:

$$\Delta t = \frac{2\pi}{\omega} \quad (3)$$

Following Eq. (1), mutation times referring to the properties $g = G'$ and $g = G''$ can be written as:

$$\tau'_{mu} = \left[\frac{1}{G'}\left|\frac{\partial G'}{\partial t}\right|\right]^{-1} \quad \text{and} \quad \tau''_{mu} = \left[\frac{1}{G''}\left|\frac{\partial G''}{\partial t}\right|\right]^{-1} \quad (4a) \text{ and } (4b)$$

Correspondingly, mutation numbers need to be calculated separately for $G'(\omega)$ and $G''(\omega)$:

$$N'_{mu} = \frac{2\pi}{\omega G'}\left|\frac{\partial G'}{\partial t}\right| \quad \text{and} \quad N''_{mu} = \frac{2\pi}{\omega G''}\left|\frac{\partial G''}{\partial t}\right| \quad (5a) \text{ and } (5b)$$

In order to consider the sample quasi-stable during the experimental time, both of these mutation numbers need to be sufficiently small, $N_{mu} << 1$. Winter et al. (1988) found, for instance, that nonlinear effects were negligible in a gelation experiment when $N_{mu} < 0.15$. On the other hand, Mours and Winter (1994) determined a critical mutation number of $N_{mu} < 0.9$ for a constant heating rate experiment, and Pogodina and Winter (1998) considered samples with $N_{mu} \leq 0.3$ as quasi-stable during crystallization. It is worth noting that G' usually changes more rapidly than G'' in mutating samples, and therefore $N'_{mu} > N''_{mu}$ (Mours and Winter 1994; Winter et al. 1998).

Two types of rheological experiments can be used to produce data for TRR analysis: cyclic frequency sweeps (CFS) and Fourier transform mechanical spectroscopy (FTMS). In the CFS protocol, a frequency sweep experiment is repeated in a continuous fashion for a long period of time. On the contrary, FTMS allows the probing of the material at several angular frequencies simultaneously, reducing the duration of a rheological experiment as compared to the CFS protocol (Holly et al. 1988). The frequency resolution of this method, however, is often limited by the linear viscoelastic (LVE) domain of the material and the sensitivity of the measuring device (Ghiringhelli et al. 2012). These limitations are particularly critical for glassy materials that have very narrow LVE regime. Consequently, although many commercial rheometer models are capable of performing FTMS experiments, the more simple and accurate CFS method is a preferred way to produce data for the TRR analysis of physical aging.

Advantages of TRR over the Struik's protocol

In the so-called Struik's protocol, the material sample is subjected to successive creep and recovery experiments during physical aging (Struik 1966, 1977). In order to limit sample mutation effects to an acceptable level during the creep measurements, each creep period is kept short in comparison with the previous aging time as well as the last recovery period preceding it. The Struik's protocol is by far the most commonly used mechanical test method to study physical aging in amorphous and semi-crystalline polymers, as well as in other glassy materials.

It is notable that TRR has several advantages over the Struik's protocol as a mechanical characterization method of physical aging:

- Frequency sweep data used in the TRR analysis is more informative (i.e. provides more comprehensive description of the linear viscoelastic behavior of a material) than creep data obtained by the Struik's protocol. In particular, frequency sweep experiments probe both slow and fast time scales of the material.
- The Kramers-Kronig relation (Kronig 1926; Kramers 1927)

$$\frac{G'(\omega)}{\omega^2} = \frac{2}{\pi}\int_0^\infty \frac{G''(x)}{\omega^2 - x^2}\,\mathrm{d}x \tag{6}$$

  allows a consistency check on the frequency sweep data employed in the TRR analysis; i.e., the quality of *G'* and *G''* data can be readily assessed (Booij and Thoone 1982; Winter 1997).
- TRR allows continuous monitoring of the rheological properties during physical aging, whereas data can be collected only at discrete aging times in the Struik's protocol.
- Based on our experience, if a rotational rheometer is used to measure rheological data during physical aging (as in the Experimental section of this paper), it is easier to obtain good dynamic oscillatory data than good creep data.

Time-aging time superposition

The evolution of rheological response during physical aging is often analyzed by time-aging time superposition, a concept similar to the well-known time-temperature superposition principle (Struik 1977; Bradshaw and Brinson 1997). In this method, horizontal (and in some cases also vertical) shifting is used to construct master curves of rheological data measured at different aging times. This approach is equally applicable to the analysis of the dynamic viscoelastic data produced by the TRR method and to the analysis of the creep data produced by the Struik's protocol. It can be seen then that, if successful, the time-aging time superposition principle is a powerful tool for the estimation of material response at long loading times from tests conducted over relatively short timescales (Brinson and Gates 1995; Joshi 2014).

As a result of the master curve construction, one obtains aging time shift factors a_{te} (and vertical shift factors b_{te}, if appropriate) as a function of aging time. A power-law dependence of a_{te} on aging time t_e is often experimentally observed (and theoretically predicted for polymer glasses (Chen and Schweizer 2007)). The slope in the log-log plot of a_{te} vs. t_e is defined as the aging shift rate μ (Struik 1977):

$$\mu = \frac{d \log a_{te}}{d \log t_e} \tag{7}$$

μ is temperature- and material-dependent and is typically limited to values of $\mu \leq 1$ (Struik 1977). At long aging times, however, the increase in a_{te} becomes slower, and eventually a_{te} reaches a plateau. This plateau can be considered as an indication of the equilibrium mechanical response where physical aging has completely ceased (O'Connell and McKenna 1999).

Experimental

In this investigation, TRR is employed to characterize physical aging in bituminous binders. Some basic properties of the investigated binder samples are given in Table 1. Neat bitumen samples A and B were used to study the effects of crystallinity and temperature on physical aging. The crystallinity difference between these two bitumen samples is demonstrated by the heat flow curves of Fig. 1. In addition, bitumen C was blended with different amounts (3-10 wt%) of star-branched styrene-butadiene-styrene (SBS) triblock copolymer (Calprene 411, M_n = 311 kg/mol, M_w/M_n = 1.11, styrene content = 30 wt%) to study the effect of polymer modification on physical aging. More information about these SBS modified bitumen samples is provided elsewhere (Laukkanen et al. 2018a).

Table 1 Overview of the properties of the investigated bituminous binders.

	Pen at 25 °C [1/10mm] [a]	$T_{R\&B}$ [°C] [b]	$T_{g,onset}$ [°C] [c]	$T_{g,mid}$ [°C] [c]	$T_{g,end}$ [°C] [c]	ΔH_m [J/g] [c]
Bitumen A	80	45.8	-43.7	-23.9	-4.2	7.1
Bitumen B	64	47.7	-32.5	-19.7	-6.7	0.0
Bitumen C	177	38.4	-35.6	-18.7	-1.8	3.5
Bitumen C + 3 wt% SBS	107	59.0	-35.4	-19.4	-3.6	3.4
Bitumen C + 5 wt% SBS	79	98.5	-35.4	-19.8	-4.3	3.1
Bitumen C + 7 wt% SBS	64	103.5	-36.2	-20.7	-5.3	2.4
Bitumen C + 10 wt% SBS	50	112.5	-35.7	-21.1	-6.7	1.3

[a] The needle penetration (Pen) at 25 °C was measured according to EN 1426

[b] The Ring-and-Ball softening point ($T_{R\&B}$) was measured according to EN 1427

[c] The glass transition temperatures ($T_{g,onset}$, $T_{g,mid}$, $T_{g,end}$) and the melting enthalpy (ΔH_m) were determined by differential scanning calorimetry (DSC). $T_{g,mid}$ is defined as the temperature at the half-height of the heat capacity step associated with the glass transition. See Fig. 1 of this article and Fig. 3 of Laukkanen et al. (2018a) for the graphical determination of these parameters.

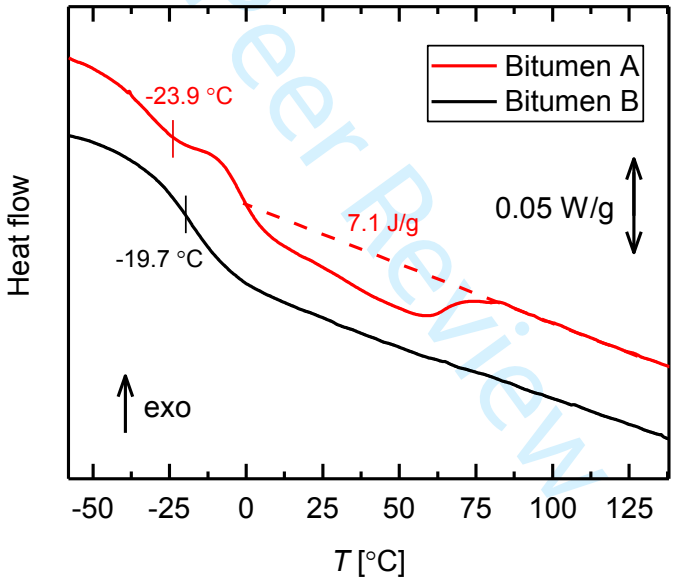

Fig. 1 Heat flow curves of bitumen samples A and B, measured at a heating rate of 10 K/min. The glass transition temperatures (the midpoints of the glass transition region) are denoted in the figure, as well as the area of the endotherm that corresponds to the melting enthalpy of Bitumen A.

Rheological experiments were carried out with a stress-controlled Malvern Kinexus Pro rheometer. The temperature of the test specimen was controlled within ±0.1 K by a Peltier plate and active hood, connected to a Julabo CF41 refrigerated circulator. In order to avoid torsional instrument compliance effects caused by high sample stiffness (Schröter et al. 2006), a parallel plate geometry with a small diameter of 4 mm was employed in the measurements. The accuracy and reliability of this measurement technique, commonly known as small-diameter

parallel plate (SDPP) rheometry, have been demonstrated in a separate paper (Laukkanen 2017).

Rheological test specimens were prepared for the measurement by placing sufficient amount of material on the lower plate of the rheometer that was preheated to ~10 K above the Ring-and-Ball softening point of the bitumen sample. The specimen was carefully trimmed at a gap height of 1.87 mm, after which the gap was further decreased to 1.75 mm. Finally, the specimen was cooled to the measurement temperature at the maximum cooling rate of the rheometer temperature control system (approximately 10 K/min on average), and the specimen temperature was allowed to equilibrate for about 500 s before starting the experiment.

The evolution of the dynamic viscoelastic properties (G', G'', tan δ) during physical aging was monitored by performing cyclic frequency sweep (CFS) experiments. The frequency range from 10 to 0.1 Hz (ω = 62.8 to 0.628 rad/s) was repeatedly scanned while keeping the temperature constant. The strain amplitude was kept low (γ_0 = 0.01 – 0.03 % depending on the measurement temperature) in order to ensure linear viscoelastic material response and to ensure that physical aging is not influenced by mechanical rejuvenation. During the measurement, the Peltier hood was purged with dry nitrogen gas to avoid moisture uptake and ice formation in the test specimen, and the rheometer normal force control was enabled to account for possible volume changes in the test specimen. All measurement data were corrected for the instrument compliance using the procedure described in Laukkanen (2017).

Results and discussion

Fig. 2 shows the evolution of the dynamic viscoelastic properties of Bitumen A during physical aging at the calorimetric T_g. The total duration of this experiment was approximately 7.4×10^5 s or 8.6 days. The zero time is defined as the moment when the rheometer reached the measurement temperature. After this, additional 510 s were waited prior to initiating the CFS experiment in order to ensure that the test specimen is in thermal equilibrium. Notably, a substantial increase in G' is observed with aging time. This increase appears to follow a similar trend at all measurement frequencies, the curves being substantially parallel to each other. It is also interesting to note that, at intermediate aging times, these curves are fairly linear (when plotted as a function of the logarithm of aging time). Similar aging time dependences of G' (or E') have been found in various polymer glasses such as polyvinyl acetate (Kovacs et al. 1963), poly(arylene etherimide) (Brennan and Feller III 1995), poly (methyl methacrylate) (Venditti and Gillham 1992b), Tritan copolyester (Cugini and Lesser 2015), and poly(2,6-dimethyl-l,4-phenylene oxide)-polystyrene (PPO-PS) blends (Cavaille et al. 1986). At long aging times, the aging process slows down and eventually ceases as G' reaches a plateau. As could be expected, the time to reach this plateau is independent of the measurement frequency and is on the order of 10^5 s (≈28 h). This finding is in fair agreement with the results of Lu and Isacsson (2000) which indicate that the physical aging of bitumen typically persists for 1-2 days in the temperature range of -15 to -35 °C. On the other hand, G'' shows only weak dependences on the aging time and measurement frequency at T_g It is also worth noting that the loss tangent,

tan $\delta = G''/G'$, decreases significantly with aging time, reflecting the increasing dominance of elastic properties over viscous ones.

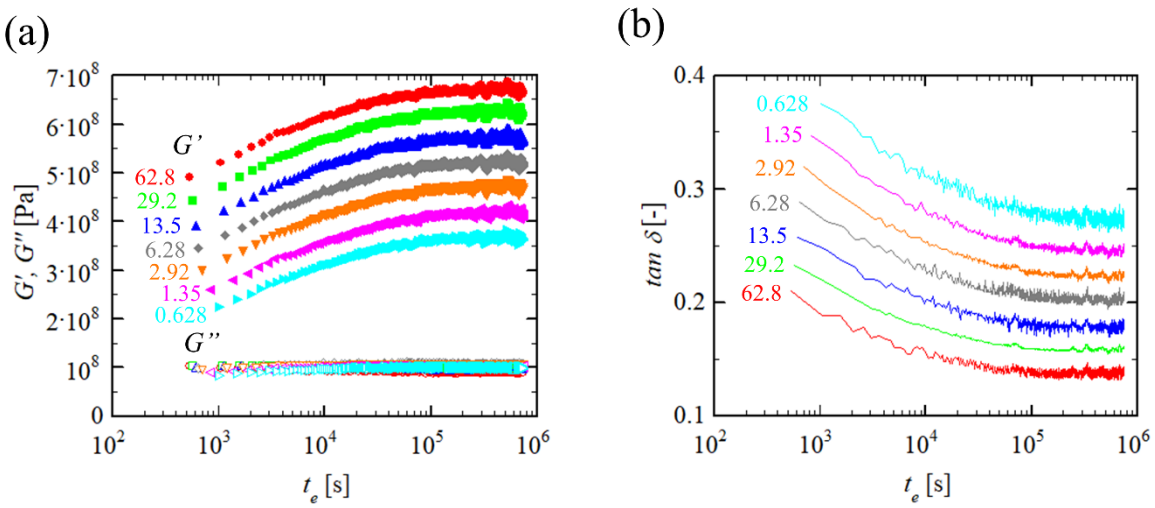

Fig. 2 Evolution of frequency-dependent (a) dynamic moduli and (b) loss tangent during physical aging of Bitumen A at T_g = -23.9 °C. Zero time is defined as the moment when the Peltier plate of the rheometer reaches the measurement temperature. The temperature of the test specimen was allowed to equilibrate for 510 s before starting to collect CFS data.

Furthermore, mutation numbers N'_{mu} corresponding to the G' data of Fig. 2 were calculated. As discussed above, the time evolution in G'' values is negligible compared to the time evolution in G' values, and it is therefore sufficient to analyze N'_{mu} values in this case ($N'_{mu} >> N''_{mu}$). Fig. 3 shows that N'_{mu} decays exponentially at short aging times and approaches zero very fast after the initiation of physical aging. Even at short aging times, sample mutation is very slow ($N'_{mu} < 0.0023$) at all measurement frequencies. Moreover, N'_{mu} decreases strongly with increasing measurement frequency as the experimental time Δt becomes longer, cf. Eq. (3). Based on the above observations, it is safe to say that sample mutation does not pose limitations to the TRR analysis of physical aging, meaning that the sample can be considered quasi-stable during the experimental time. This is indeed not surprising as physical aging is generally viewed as a much slower process than most other time-dependent material transitions such as gelation and crystallization.

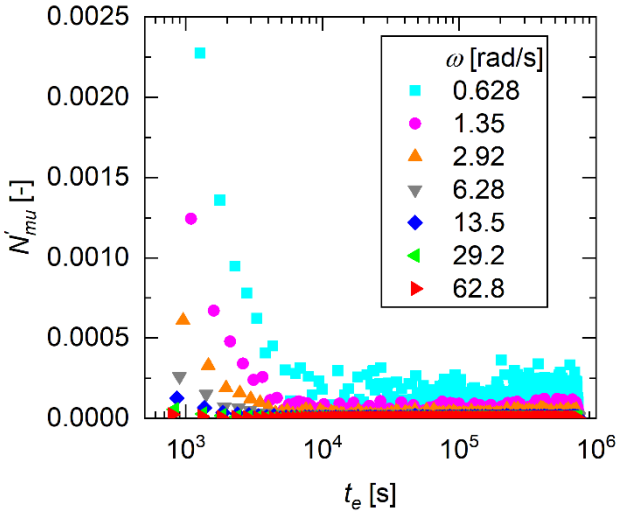

Fig. 3 Mutation number versus aging time for the frequency-dependent storage modulus data of Fig. 2(a).

To further analyze the CFS data of Fig. 2, interpolated frequency sweep data at various instances during physical aging is shown in Fig. 4(a) (see Mours and Winter (1994) for the details of the interpolation procedure). This figure again demonstrates the increase in *G'* with aging time and the almost constant value of *G''*. Fig. 4(b) shows the master curves constructed from the frequency sweep data of Fig. 4(a) using the time-aging time superposition principle. The lines in this figure represent the fits of the generalized Maxwell model to the experimental data, resulting from the calculation of the relaxation time spectrum by the method of Baumgärtel and Winter (1989). The close agreement between these model fits and the experimental data proves that the experimental data satisfies the Kramers-Kronig relation, Eq. (6), which in turn indicates good data quality (Winter 1997). Furthermore, Fig. 4(c) depicts the aging time shift factors that were used to obtain the master curves of Fig. 4(b). Note that only horizontal shifts were used, vertical shifts were not necessary. As expected, the logarithm of the aging time shift factor shows a linear dependence on the logarithm of the aging time at the early stages of physical aging, the slope being $\mu \approx 0.60$. It is also noted that, similarly to Fig. 2, the plateauing of aging time shift factors indicates the completion of physical aging after approximately 10^5 s (≈28 h).

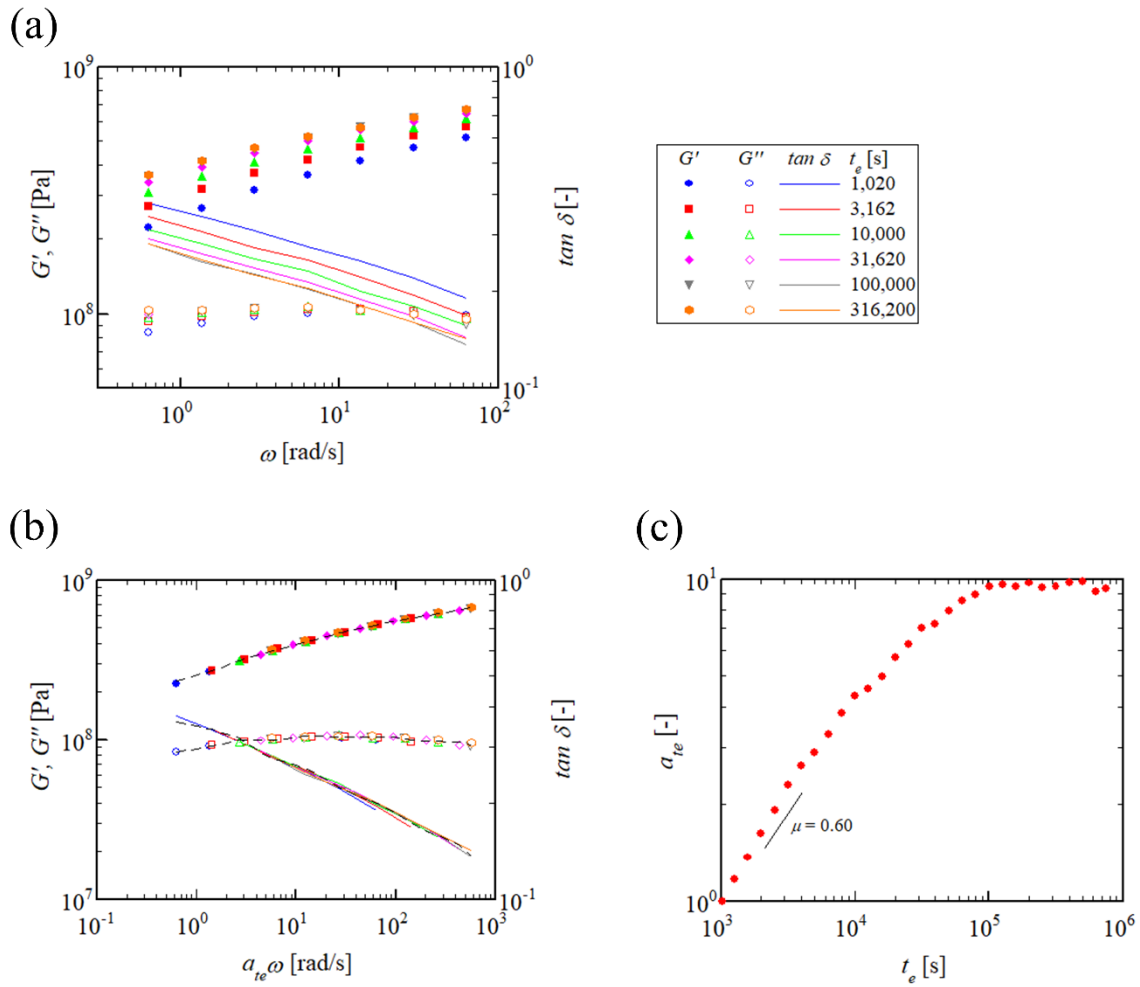

Fig. 4 Application of the time-aging time superposition principle to the physical aging data of Bitumen A. (a) Frequency sweep response at different stages of physical aging, interpolated from the CFS data of Fig. 2. (b) Master curves obtained by horizontally shifting the frequency sweep data of part (a). The excellent fit of the Generalized Maxwell model (dashed line) to the experimental data proves that the Kramers-Kronig relation is satisfied, thus indicating good data quality. (c) Aging time shift factors used to construct the master curves of part (b).

The temperature dependence of the rate of physical aging in Bitumen A is demonstrated in Fig. 5. In addition to the above described experiment at the calorimetric T_g (-23.9 °C), CFS experiments were performed at four different temperatures ranging from T_g+10 K (-13.9 °C) to T_g-10 K (-33.9 °C). In these additional measurements, dynamic viscoelastic properties were monitored over a time period of approximately 10^5 s (≈28 h). This shorter test duration did not, unfortunately, allow us to detect the state of complete physical aging at temperatures of T_g+10 K, T_g+5 K, T_g-5 K and T_g-10 K. Nonetheless, these experiments provided us information about physical aging behavior in the power-law aging regime (where μ = log a_{te} / log t_e is roughly constant). It is observed that physical aging rates are significant both above and below the nominal T_g of -23.9 °C, μ values varying in the range of about 0.40 to 0.60. Although the variations in the aging shift rate are relatively small in the investigated temperature range, it may be noted that the rate of physical aging appears to be highest at T_g or very close to it (μ_{T_g} ≈ 0.60), while decreasing at temperatures further away from T_g ($\mu_{T_g+10\,K} \approx \mu_{T_g-10\,K} \approx 0.40$). This

observation is consistent with the results of Planche et al. (1998) and Tabatabaee et al. (2012) who studied the temperature dependence of physical aging in a total of 55 bituminous binders by means of bending beam rheometer (BBR) measurements. In comparison with other small-molecule glass-forming liquids, aging shift rates of similar order of magnitude have been reported for *m*-toluidine ($\mu = 0.50$), glycerol ($\mu = 0.38$) and sucrose benzoate ($\mu = 0.25$) at T_g-6 K (Hutcheson and McKenna 2008).

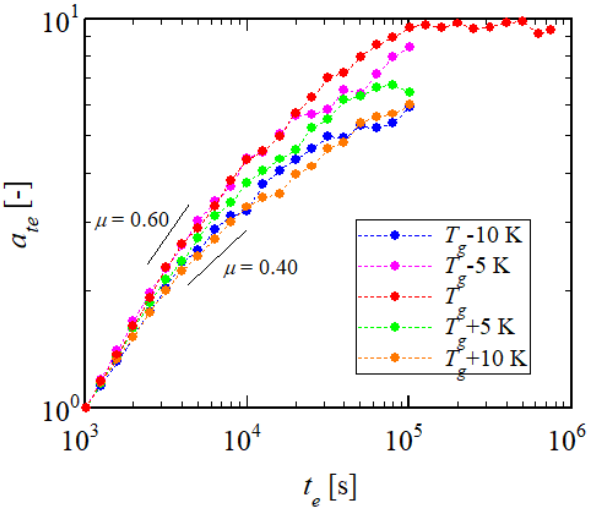

Fig. 5 Temperature dependence of the aging time shift factors for Bitumen A.

It is also worth emphasizing that, unlike bitumen, most glassy materials exhibit physical aging only below T_g (Struik 1977). We suggest that the unusual property of bitumen to physically age above the nominal T_g is due to its broad glass transition. This is evidenced by the fact that the glass transition region of Bitumen A, as measured by DSC (Table 1), extends to temperatures far outside the temperature range covered by our physical aging experiments (T_g+10 K to T_g-10 K, T_g being the midpoint of the glass transition region). Earlier studies (Masson and Polomark 2001; Masson et al. 2002; Laukkanen et al. 2018c, b) have suggested that the broad glass transition of bitumen originates from the chemical and structural complexity of this material. Consequently, it can be speculated that molecular constituents responsible for the high-temperature side of the bitumen glass transition are also responsible for the physical aging above the nominal (midpoint) T_g.

Fig. 6 shows a summary of the results from the physical aging experiments on Bitumen B. When comparing Fig. 6(a) with Fig. 4(a), it is apparent that physical aging is much less severe in non-waxy Bitumen B than in waxy Bitumen A. Still, as shown in Fig. 6(b), the time-aging time superposition principle is valid for Bitumen B, allowing the construction of master curves from the frequency sweep data obtained at different stages of physical aging. In this case, only small horizontal shifts are needed to generate these master curves. This is further illustrated in Fig. 6(c) where aging time shift factors are plotted against aging time. Only minor physical aging is observed to take place in Bitumen B over the entire experimental temperature range from T_g+30 K (10 °C) to T_g-20 K (-40 °C). It can therefore be concluded that crystallinity has a major effect on the rate of physical aging in bitumen, and this effect can be readily detected by TRR. The correlation between crystallinity and physical aging of bitumen has been

identified also by several other researchers (Claudy et al. 1992; Anderson et al. 1994; Planche et al. 1998; Anderson and Marasteanu 1999).

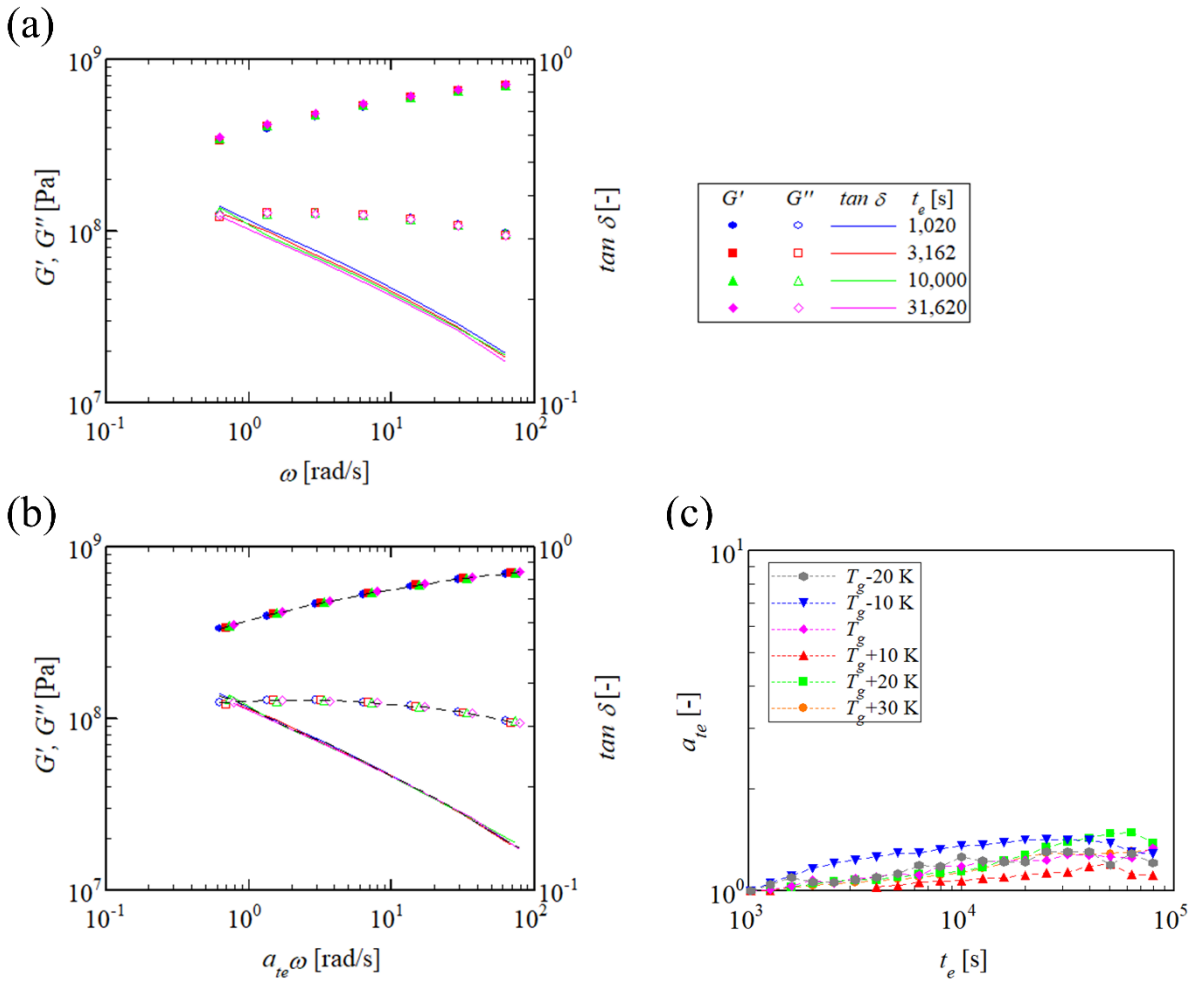

Fig. 6 Application of the time-aging time superposition principle to the physical aging data of Bitumen B. (a) Interpolated frequency sweep response during physical aging at T = -20 °C ≈ T_g. (b) Master curves obtained by horizontally shifting the frequency sweep data of part (a). The excellent fit of the Generalized Maxwell model (dashed line) to the experimental data proves that the Kramers-Kronig relation is satisfied, thus indicating good data quality. (c) Temperature dependence of the aging time shift factors for Bitumen B. The same scaling is used as in Fig. 4(c) for the ease of comparison.

As the final case, we investigate the effect of SBS polymer modification on the physical aging of bitumen. Fig. 7(a) shows interpolated frequency sweep data at selected aging times for a highly polymer-modified Bitumen C + 10 wt% SBS. Interestingly, the loss tangent of Bitumen C + 10 wt% SBS appears to be almost independent of the frequency at all aging times, and consequently *G'* and *G''* curves are nearly parallel to each other. This is characteristic of critical gel-like behavior as first observed by Chambon and Winter (1985, 1987; 1986). It can be speculated that this type of viscoelastic behavior originates from the fractal morphology of SBS modified bitumen as suggested by Jelčić and coworkers (2016; 2017). The time-aging

time superposition is found to be valid at all SBS concentrations (0, 3, 5, 7 and 10 wt%) as exemplified in Fig. 7(b) for the two of the samples.

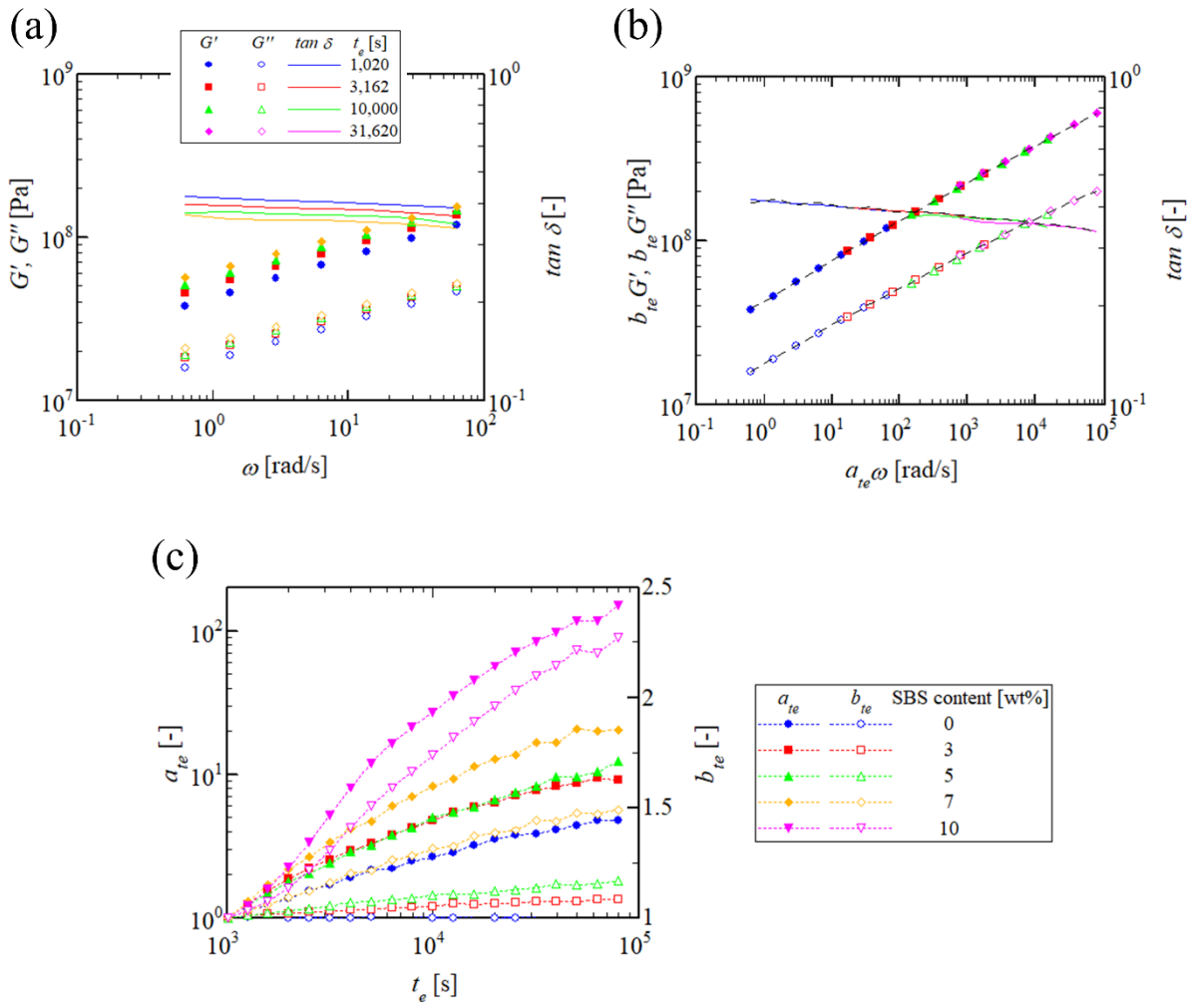

Fig. 7 Application of the time-aging time superposition principle to the physical aging data of SBS modified bitumen. (a) Interpolated frequency sweep response of Bitumen C + 10 wt% SBS during physical aging at T = -20 °C ≈ T_g. (b) Master curves obtained by horizontally and vertically shifting the frequency sweep data of part (a). The excellent fit of the Generalized Maxwell model (dashed line) to the experimental data proves that the Kramers-Kronig relation is satisfied, thus indicating good data quality. (c) SBS polymer concentration dependence of horizontal and vertical time-aging time shift factors.

Furthermore, the aging time shift factors obtained from the time-aging time superposition are depicted in Fig. 7(c). It is observed that only horizontal shifts are needed to construct master curves for the bitumen samples that have been modified with small amounts (≤5 wt%) of SBS. On the contrary, both horizontal and vertical shifts need to be employed in order to obtain smooth master curves for the bitumen samples modified with 7 and 10 wt% of SBS. We have previously observed that a continuous SBS-rich network is formed within these highly SBS modified bitumen samples and that they exhibit thermorheologically complex behavior (Laukkanen et al. 2018a). Consequently, it can be speculated that the formation of the

polymeric network structure gives rise to the vertical shifts upon physical aging. Further studies are needed to confirm and further explain this hypothesized relation.

Fig. 7(c) also shows that the aging time shift factors increase significantly with increasing SBS content, resulting in an apparent increase in μ values. Following the traditional interpretation, this would indicate that SBS modification increases the rate of physical aging. It should be noted, however, that it is not meaningful to use only μ values to assess the extent of physical aging in SBS modified bitumen. This is because the rheological properties of SBS modified bitumen show much weaker frequency dependence than those of unmodified bitumen, and consequently similar changes in rheological properties result in considerably larger time-aging time shifts in SBS modified bitumen than in unmodified bitumen. In fact, SBS modification does not appear to have any significant influence on physical aging induced stiffening; i.e. relative increases in the modulus values are observed to be almost independent of the SBS concentration.

Conclusion

We have shown that time-resolved rheometry (TRR) is a useful tool to monitor changes in viscoelastic properties during physical aging. The TRR technique is used to analyze cyclic frequency sweep (CFS) data, providing many advantages over the traditional Struik's physical aging test protocol. In the experimental section of this paper, physical aging in bituminous binders is investigated. To the best of authors' knowledge, this is the first time that the TRR technique has been employed to study physical aging in small-molecule (non-polymeric) glass-forming liquids. The mutation of viscoelastic properties is verified to be relatively slow during physical aging ($N'_{mu} << 1$), thus allowing rheological measurements in the quasi-stable state. As a proof of concept, the effects of temperature and crystallinity on the physical aging of bitumen have been quantified. The time-aging time superposition is found to be valid for unmodified as well as for SBS polymer modified binders. Interestingly, only horizontal time-aging time shifts are needed to generate master curves for unmodified and moderately SBS modified binders, whereas both horizontal and vertical shifts are necessary in the case of highly SBS modified binders. Further studies are needed to explain the physical origin of this divergence. Future studies are also expected to extend the application of the presented analysis techniques to other types of glass-forming liquids.

Acknowledgement

O.V.L. gratefully acknowledges financial support from Osk. Huttunen Foundation and Nynas AB.

References

Alcoutlabi M, Martinez-Vega JJ (1999) Effect of physical ageing on the relaxation time spectrum of amorphous polymers: The fractional calculus approach. J Mater Sci 34:2361–2369. doi: 10.1023/A:1004546228825

Anderson D, Marasteanu M (1999) Physical Hardening of Asphalt Binders Relative to Their Glass Transition Temperatures. Transp Res Rec J Transp Res Board 1661:27–34. doi: 10.3141/1661-05

Anderson DA, Christensen DW, Bahia HU, et al (1994) Binder characterization and evaluation. Volume 3: Physical characterization. Strategic Highway Research Program

Araki O, Horie M, Masuda T (2001a) Physical Aging of Polycarbonate Investigated by Dynamic Viscoelasticity. J Polym Sci Part B Polym Phys 39:337–341. doi: 10.1002/1099-0488(20010201)39:3<337::AID-POLB1006>3.0.CO;2-N

Araki O, Masuda T (2001) Role of a small amount of comonomer on the physical aging of poly(methyl methacrylate) copolymer investigated by dynamic viscoelasticity. Polymer 43:857–861. doi: 10.1016/S0032-3861(01)00638-3

Araki O, Shimamoto T, Yamamoto T, Masuda T (2001b) Physical aging of polystyrene investigated by dynamic viscoelasticity. Polymer 42:4433–4437. doi: 10.1016/S0032-3861(00)00830-2

Bahia H, Tabatabaee H, Velasquez R (2012) Importance of bitumen physical hardening for thermal stress buildup and relaxation in asphalt. In: 5th Eurasphalt & Eurobitume Congress. pp 13–15

Baumgaertel M, Winter HH (1989) Determination of discrete relaxation and retardation time spectra from dynamic mechanical data. Rheol Acta 28:511–519. doi: 10.1007/BF01332922

Beiner M, Garwe F, Schröter K, Donth E (1994b) Ageing effects on dynamic shear moduli at the onset of the dynamic glass transition in two poly(alkyl methacrylate)s. Polymer 35:4127–4132. doi: 10.1016/0032-3861(94)90586-X

Beiner M, Garwe F, Schröter K, Donth E (1994a) Dynamic shear modulus in the splitting region of poly(alkyl methacrylates). Colloid Polym Sci 272:1439–1446. doi: 10.1007/BF00654174

Booij HC, Thoone GPJM (1982) Generalization of Kramers-Kronig transforms and some approximations of relations between viscoelastic quantities. Rheol Acta 21:15–24. doi: 10.1007/BF01520701

Bradshaw RD, Brinson LC (1997) Physical aging in polymers and polymer composites: an analysis and method for time-aging time superposition. Polym Eng Sci 37:31–44. doi: 10.1002/pen.11643

Brennan AB, Feller III F (1995) Physical aging behavior of a poly (arylene etherimide). J Rheol 39:453–470. doi: 10.1122/1.550707

Brinson LC, Gates TS (1995) Effects of physical aging on long term creep of polymers and polymer matrix composites. Int J Solids Struct 32:827–846. doi: 10.1016/0020-7683(94)00163-Q

Cavaille JY, Etienne S, Perez J, et al (1986) Dynamic shear measurements of physical ageing and the memory effect in a polymer glass. Polymer 27:686–692. doi: 10.1016/0032-

3861(86)90125-4

Chambon F, Winter HH (1985) Stopping of crosslinking reaction in a PDMS polymer at the gel point. Polym Bull 13:499–503. doi: 10.1007/BF00263470

Chambon F, Winter HH (1987) Linear Viscoelasticity at the Gel Point of a Crosslinking PDMS with Imbalanced Stoichiometry. J Rheol 31:683–697. doi: 10.1122/1.549955

Chen K, Schweizer KS (2007) Molecular theory of physical aging in polymer glasses. Phys Rev Lett 98:. doi: 10.1103/PhysRevLett.98.167802

Claudy P, Letoffe JM, Rondelez F, et al (1992) A new interpretation of time-dependent physical hardening in asphalt based on DSC and optical thermoanalysis. In: ACS Symposium on Chemistry and Characterization of Asphalts, Washington, DC

Cugini A V., Lesser AJ (2015) Aspects of physical aging, mechanical rejuvenation, and thermal annealing in a new copolyester. Polym Eng Sci 55:1941–1950. doi: 10.1002/pen.24035

De Rosa ME, Mours M, Winter HH (1997) The gel point as reference state: A simple kinetic model for crosslinking polybutadiene via hydrosilation. Polym Gels Networks 5:69–94. doi: 10.1016/S0966-7822(96)00033-0

Delin MR, Rychwalski W, Kubát J, et al (1996) Physical aging time scales and rates for poly(vinyl acetate) stimulated mechanically in the Tg-region. Polym Eng Sci 36:2955–2967. doi: 10.1002/pen.10697

Drozdov a. D, Dorfmann a. (2003) Physical aging and the viscoelastic response of glassy polymers: Comparison of observations in mechanical and dilatometric tests. Math Comput Model 37:665–681. doi: 10.1016/S0895-7177(03)00073-6

Drozdov AD (2001) The effect of temperature on physical aging of glassy polymers. J Appl Polym Sci 81:3309–3320. doi: 10.1002/app.1787

Evans M, Marchildon R, Hesp S (2011) Effects of Physical Hardening on Stress Relaxation in Asphalt Cements. Transp Res Rec J Transp Res Board 2207:34–42. doi: 10.3141/2207-05

Filippone G, Carroccio SC, Curcuruto G, et al (2015a) Time-resolved rheology as a tool to monitor the progress of polymer degradation in the melt state - Part II: Thermal and thermo-oxidative degradation of polyamide 11/organo-clay nanocomposites. Polym (United Kingdom) 73:102–110. doi: 10.1016/j.polymer.2015.07.042

Filippone G, Carroccio SC, Mendichi R, et al (2015b) Time-resolved rheology as a tool to monitor the progress of polymer degradation in the melt state–Part I: Thermal and thermo-oxidative degradation of polyamide 11. Polymer 72:134–141. doi: 10.1016/j.polymer.2015.07.042

Freeston JL, Gillespie Gh, Paliukaite M, Taylor R (2015) Physical Hardening in Asphalt. In: Proceedings of the Sixtieth Annual Conference of the Canadian Technical Asphalt Association (CTAA): Winnipeg, Manitoba

Ghiringhelli E, Roux D, Bleses D, et al (2012) Optimal fourier rheometry: Application to the gelation of an alginate. Rheol Acta 51:413–420. doi: 10.1007/s00397-012-0616-z

Guerdoux L, Duckett RA, Froelich D (1984) Physical ageing of polycarbonate and PMMA by dynamic mechanical measurements. Polymer 25:1392–1396. doi: 10.1016/0032-3861(84)90098-3

Haidar B, Smith TL (1990) Physical ageing of stretched specimens of a polycarbonate film and

its temperature dependence. Polymer 31:1904–1908. doi: 10.1016/0032-3861(90)90015-Q

Hesp SAM, Genin SN, Scafe D, et al (2009a) Five Year Performance Review of a Northern Ontario Pavement Trial: Validation of Ontario's Double-Edge-Notched Tension (DENT) and Extended Bending Beam Rheometer (BBR) Test Methods. Can Tech Asph Assoc Proc Annu Conf 54:99–126

Hesp SAM, Iliuta S, Shirokoff JW (2007) Reversible aging in asphalt binders. Energy and Fuels 21:1112–1121. doi: 10.1021/ef060463b

Hesp SAM, Soleimani A, Subramani S, et al (2009b) Asphalt pavement cracking: Analysis of extraordinary life cycle variability in eastern and northeastern Ontario. Int J Pavement Eng 10:209–227. doi: 10.1080/10298430802343169

Hodge IM (1995) Physical aging in polymer glasses. Science (80-) 267:1945–1947. doi: 10.1126/science.267.5206.1945

Holly EE, Venkataraman SK, Chambon F, Henning Winter H (1988) Fourier transform mechanical spectroscopy of viscoelastic materials with transient structure. J Nonnewton Fluid Mech 27:17–26. doi: 10.1016/0377-0257(88)80002-8

Hutcheson SA, McKenna GB (2008) The measurement of mechanical properties of glycerol, m -toluidine, and sucrose benzoate under consideration of corrected rheometer compliance: An in-depth study and review. J Chem Phys 129:. doi: 10.1063/1.2965528

Hutchinson JM (1995) Physical aging of polymers. Prog Polym Sci 20:703–760. doi: 10.1016/0079-6700(94)00001-I

Iliuta S, Andriescu A, Hesp SAM, Tam KK (2004a) Improved Approach to Low Temperature and Fatigue Fracture Performance Grading of Asphalt Cements. In: Proceedings of the Forty-Ninth Annual Conference of the Canadian Technical Asphalt Association (CTAA)-Montreal, Quebec

Iliuta S, Hesp S, Marasteanu M, et al (2004b) Field Validation Study of Low-Temperature Performance Grading Tests for Asphalt Binders. Transp Res Rec 1875:14–21. doi: 10.3141/1875-03

Jelčić Ž, Ocelić Bulatović V, Jurkaš Marković K, Rek V (2017) Multi-fractal morphology of un-aged and aged SBS polymer-modified bitumen. Plast Rubber Compos 46:77–98. doi: 10.1080/14658011.2017.1280966

Jelimir J, Bulatović VO, Rek V, Marković KJ (2016) Relationship between fractal, viscoelastic, and aging properties of linear and radial styrene-butadiene-styrene polymer-modified bitumen. J Elastomers Plast 48:14–46. doi: 10.1177/0095244314538437

Joshi YM (2014) Long time response of aging glassy polymers. Rheol Acta 53:477–488. doi: 10.1007/s00397-014-0772-4

Kaushal M, Joshi YM (2014) Validation of Effective time translational invariance and linear viscoelasticity of polymer undergoing cross-linking reaction. Macromolecules 47:8041–8047. doi: 10.1021/ma501352c

Kovacs AJ, Stratton RA, Ferry JD (1963) Dynamic Mechanical Properties of Polyvinyl Acetate in Shear in the Glass Transition Temperature Range. J Phys Chem 67:152–161. doi: 10.1021/j100795a037

Kramers HA (1927) La diffusion de la lumière par les atomes. In: Atti cong intern fisici, Transactions of Volta Centenary Congress. p 545

Kronig R de L (1926) On the theory of dispersion of x-rays. Josa 12:547–557

Kruse M, Wagner MH (2016) Time-resolved rheometry of poly(ethylene terephthalate) during thermal and thermo-oxidative degradation. Rheol Acta 55:789–800. doi: 10.1007/s00397-016-0955-2

Laukkanen O-V (2017) Small-diameter parallel plate rheometry: a simple technique for measuring rheological properties of glass-forming liquids in shear. Rheol Acta 56:661–671. doi: 10.1007/s00397-017-1020-5

Laukkanen O-V, Soenen H, Winter HH, Seppälä J (2018a) Low-temperature rheological and morphological characterization of SBS modified bitumen. Constr Build Mater 179:348–359. doi: 10.1016/j.conbuildmat.2018.05.160

Laukkanen O-V, Winter HH, Soenen H, Seppälä J (2018b) Systematic broadening of the viscoelastic and calorimetric glass transitions in complex glass-forming liquids. J Non Cryst Solids 483:10–17. doi: 10.1016/j.jnoncrysol.2017.12.029

Laukkanen O-V, Winter HH, Soenen H, Seppälä J (2018c) An empirical constitutive model for complex glass-forming liquids using bitumen as a model material. Rheol Acta 57:57–70. doi: 10.1007/s00397-017-1056-6

Lu X, Isacsson U (2000) Laboratory study on the low temperature physical hardening of conventional and polymer modified bitumens. Constr Build Mater 14:79–88. doi: 10.1016/S0950-0618(00)00012-X

Mandare P, Winter HH (2007) Shear-induced long-range alignment of BCC-ordered block copolymers. Rheol Acta 46:1161–1170. doi: 10.1007/s00397-007-0198-3

Masson JF, Polomark GM (2001) Bitumen microstructure by modulated differential scanning calorimetry. Thermochim Acta 374:105–114. doi: 10.1016/S0040-6031(01)00478-6

Masson JF, Polomark GM, Collins P (2002) Time-dependent microstructure of bitumen and its fractions by modulated differential scanning calorimetry. Energy and Fuels 16:470–476. doi: 10.1021/ef010233r

McKenna GB (2013) Physical aging in glasses and composites. In: Long-Term Durability of Polymeric Matrix Composites. pp 237–309

Mours M, Winter HH (1994) Time-resolved rheometry. Rheol Acta 33:385–397. doi: 10.1007/BF00366581

Mours M, Winter HH (1996) Relaxation patterns of nearly critical gels. Macromolecules 29:7221–7229. doi: 10.1021/ma9517097

Mours M, Winter HH (1998) Relaxation patterns of endlinking polydimethylsiloxane near the gel point. Polym Bull 40:267–274. doi: 10.1007/s002890050251

O'Connell PA, McKenna GB (1999) Arrhenius-type temperature dependence of the segmental relaxation below Tg. J Chem Phys 110:11054–11060. doi: 10.1063/1.479046

Paul Togunde O, Hesp SAM (2012) Physical hardening in asphalt mixtures. Int J Pavement Res Technol 5:46–53. doi: 10.6135/ijprt.org.tw/2012.5(1).46

Pixa R, Goett C, Froelich D (1985) Influence of deformation on the physical ageing of polycarbonate - 1. Mechanical properties near ambient temperature. Polym Bull 14:53–60. doi: 10.1007/BF00254915

Planche J., Claudy P., Létoffé J., Martin D (1998) Using thermal analysis methods to better understand asphalt rheology. Thermochim Acta 324:223–227. doi: 10.1016/S0040-

6031(98)00539-5

Pogodina N V., Winter HH (1998) Polypropylene crystallization as a physical gelation process. Macromolecules 31:8164–8172. doi: 10.1021/ma980134l

Polios IS, Soliman M, Lee C, et al (1997) Late stages of phase separation in a binary polymer blend studied by rheology, optical and electron microscopy, and solid state NMR. Macromolecules 30:4470–4480. doi: 10.1021/ma9701292

Ricco T, Smith TL (1990) Rate of physical aging of polycarbonate at a constant tensile strain. J Polym Sci Part B Polym Phys 28:513–520. doi: 10.1002/polb.1990.090280406

Salehiyan R, Malwela T, Ray SS (2017) Thermo-oxidative degradation study of melt-processed polyethylene and its blend with polyamide using time-resolved rheometry. Polym Degrad Stab 139:130–137. doi: 10.1016/j.polymdegradstab.2017.04.009

Schröter K, Hutcheson SA, Shi X, et al (2006) Dynamic shear modulus of glycerol: Corrections due to instrument compliance. J Chem Phys 125:214507. doi: 10.1063/1.2400862

Simon SL (2001) Aging, physical. In: Encyclopedia of Polymer Science and Technology. Wiley Online Library

Soenen H, Ekblad J, Lu X, Redelius P (2004) Isothermal hardening in bitumen and in asphalt mix. In: Eurasphalt & Eurobitume Congress Vienna. pp 1364–1375

Struik LCE (1966) Volume relaxation in polymers. Rheol Acta 5:303–311. doi: 10.1007/BF02009739

Struik LCE (1977) Physical aging in amorphous polymers and other materials. Ph.D. thesis, Delft University of Technology

Tabatabaee HA, Velasquez R, Bahia HU (2012) Predicting low temperature physical hardening in asphalt binders. Constr Build Mater 34:162–169. doi: 10.1016/j.conbuildmat.2012.02.039

Tian F, Luo Y, Yin S, et al (2015) Dynamic viscoelastic properties of polyvinyl chloride with physical aging. Korea-Australia Rheol J 27:259–266. doi: 10.1007/s13367-015-0026-8

Venditti RA, Gillham JK (1992a) Physical aging deep in the glassy state of a fully cured polyimide. J Appl Polym Sci 45:1501–1516. doi: 10.1002/app.1992.070450901

Venditti RA, Gillham JK (1992b) Isothermal physical aging of poly(methyl methacrylate): Localization of perturbations in thermomechanical properties. J Appl Polym Sci 45:501–506. doi: 10.1002/app.1992.070450314

Wang SF, Ogale AA (1989) Effects of physical aging on dynamic mechanical and transient properties of polyetheretherketone. Polym Eng Sci 29:1273–1278. doi: 10.1002/pen.760291810

Winter HH (2016) Gel Point. In: Encyclopedia of Polymer Science and Technology. pp 1–15

Winter HH (1997) Analysis of dynamic mechanical data: inversion into a relaxation time spectrum and consistency check. J Nonnewton Fluid Mech 68:225–239. doi: 10.1016/S0377-0257(96)01512-1

Winter HH, Chambon F (1986) Analysis of Linear Viscoelasticity of a Crosslinking Polymer at the Gel Point. J Rheol 30:367–382. doi: 10.1122/1.549853

Winter HH, Morganelli P, Chambon F (1988) Stoichiometry effects on rheology of model polyurethanes at the gel point. Macromolecules 21:532–535. doi: 10.1021/ma00180a048